

Online Brain Tissue Classification in Multiple Sclerosis using a Scanner-integrated Image Analysis Pipeline

Refaat E. Gabr¹, Amol Pednekar², Xiaojun Sun¹ and Ponnada A. Narayana¹

¹*Department of Diagnostic and Interventional Imaging, University of Texas Health Science Center at Houston, Houston, TX, U.S.A.*

²*Philips Healthcare, Cleveland, OH, U.S.A.*

Keywords: Multiple Sclerosis, White Matter Lesions, Segmentation, Online Processing.

Abstract: With recent advances in the field, magnetic resonance imaging (MRI) has become a powerful quantitative imaging modality for the study of neurological disorders. The quantitative power of MRI is significantly enhanced with multi-contrast and high-resolution techniques. However, those techniques generate large volumes of data which, combined with the sophisticated state-of-the-art image analysis methods, result in a very high computational load. In order to keep the scanner workflow uninterrupted, processing has to be performed off-line leading to delayed access to the quantitative results. This time delay also precludes the evaluation of data quality, and prevents the care giver from using the results of quantitative analysis to guide subsequent studies. We developed a scanner-integrated system for fast online processing of dual-echo fast spin-echo and fluid-attenuated inversion recovery images to quickly classify different brain tissues and generate white matter lesion maps in patients with multiple sclerosis (MS). The segmented tissues were imported back into the patient database on the scanner for clinical interpretation by the radiologist. The analysis pipeline included rigid-body registration, skull stripping, nonuniformity correction, and tissue segmentation. In six MS patients, the average time taken by the processing pipeline to the final segmentation of the brain into white matter, grey matter, cerebrospinal fluid, and white matter lesions was ~2 min, making it feasible to generate lesion maps immediately after the scan.

1 INTRODUCTION

Multiple sclerosis (MS) is an inflammatory demyelinating disease of the central nervous system. MS affects 2-2.5 million people world-wide, and primarily affects females and young adults between 20-50 years (Milo and Kahana, 2010). Although MS is not considered a fatal disease, MS patients struggle to lead productive lives. The annual health care cost per patient is estimated to be around \$47,215, including the lost productivity (Kobelt et al., 2006).

MRI is the most sensitive imaging modality for MS, and is a key element in the diagnosis and management of MS (Sahraian and Eshaghi, 2010). Focal white matter (WM) inflammation, the hallmark of MS, is detected on MRI as hypointensity on T1-weighted MRI, as enhancing areas following the injection of a contrast agent, or as hyper-intensity on T2-weighted and fluid-attenuated inversion recovery (FLAIR) MRI. MRI enables

assessing WM lesion load, which is an important measure in monitoring disease progression (Popescu et al., 2013; Fisniku et al., 2008; Caramanos et al., 2012).

MS lesions can be segmented on MRI images using fully automated techniques (e.g. (Sweeney et al., 2013; Karimaghloo et al., 2012) and (Datta and Narayana, 2013)). However, image analysis consists of multiple computationally intensive and time-consuming operations, and the lesion map is typically available only after the patient has left the scanner area. The lack of fast quantitative analysis prevents the technologist or physician from quickly previewing the quantitative MRI metrics of the disease or evaluating the data quality in the context of the generated quantitative measures. Moreover, the time delay precludes the prescription or the optimization of the following scans that could benefit from the availability of prior lesion segmentation.

The image processing and analysis techniques

for detecting WM lesions in MS include the following steps. First, all datasets are co-registered using a suitable registration technique. Second, the extra-meningeal tissues are removed (often called skull stripping or brain extraction). Third, images are corrected for intensity variations due to field nonuniformity. Finally, image segmentation is used to classify brain tissue into WM, grey matter (GM), cerebrospinal fluid (CSF), and WM lesions. It is worth noting that the order of some processing operation may change and certain operations could be combined together in order to make the analysis robust against certain artefacts.

With the large number of voxels generated in MRI, many of these processing operations are computationally intensive and very time consuming, and performing these operations on the scanner computer could significantly affect the scanner's functionality. Consequently, image analysis is typically performed off-line after the scan session. We recognize a critical need for a framework that can process MRI data in almost real-time to provide quantitative brain tissue and lesion maps immediately after the scan, and without affecting the scanner's performance. Eliminating the time gap between image acquisition and tissue and lesion quantification will also allow localized analysis of the lesions using specialized acquisitions (e.e. MR spectroscopy or high-resolution techniques) for improved diagnostic accuracy. In this report we describe an optimized framework wherein a fast image analysis pipeline is integrated into a clinical MRI system for online segmentation of various brain tissues in MS patients.

2 METHODS

2.1 MRI Acquisition Protocol

Images from six MS patients were processed for tissue classification and T2-hyperintense lesion detection (other MS lesions can be analysed in a similar fashion). All experiments were done on a Philips Achieva 3.0 T system (Philips Healthcare, Best, The Netherlands). The MRI protocol for MS patients included the acquisition of multi-slice (44-slices) fat-saturated dual-echo fast spin-echo (FSE) sequence with $TR/TE1/TE2 = 6800/8.2/90$ msec, $FOV = 256 \times 256 \times 132$ mm³, voxel size = $1.00 \times 1.22 \times 3.00$ mm³, scan time 3:24, and multi-slice FLAIR with $TR/TI/TE = 10000/2600/80$ msec, $FOV = 256 \times 256 \times 132$ mm³, voxel size = $1 \times 1 \times 3$ mm³, scan time 4:20. The dual-echo FSE and FLAIR images

were reconstructed to the same matrix size ($256 \times 256 \times 44$). The short-echo signal of the dual-echo FSE is proton density (PD) weighted, while the long-echo signal is T2 weighted (T2W).

2.2 System Layout

MRI data analysis was performed on a dedicated processing workstation (Quad-Core Intel Xeon E5640 2.66 GHz with 3.25 GB of memory, running on Windows XP) connected to the scanner computer through a fast network link. Special software modules were added to the scanner console to extract data from the patient database into a vendor-specific compact image format. The data were transferred to the processing workstation using a HTTP protocol (hypertext transfer protocol).

Image processing and analysis were performed on the workstation using a custom software package written in the interactive data language (IDL, Exelis Visual Information Solutions, Boulder, CO), Matlab (The Mathworks, Natick, MA), and C programming languages. The segmentation results were exported to the scanner computer and added to the patient database (Fig. 1). The segmented images were available for preview by the technologist or physician, and for review by the radiologist to aid the diagnosis. Data transfer to the workstation, image analysis, and importing data into the patient's database were all fully automated and integrated with the MRI scanner in a seamless way, without the need for user interaction.

2.3 Analysis Pipeline

The processing steps performed on the dual-echo FSE and FLAIR datasets are summarized in Fig. 2. First, the FLAIR dataset was co-registered with the dual-echo data using a rigid-body transformation (Collignon et al., 1995) in SPM8 software (Wellcome Department of Cognitive Neurology, London, UK). Second, extra-meningeal tissues were

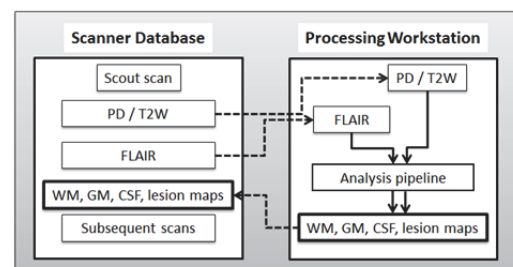


Figure 1: Online system for tissue classification and lesion segmentation in MS.

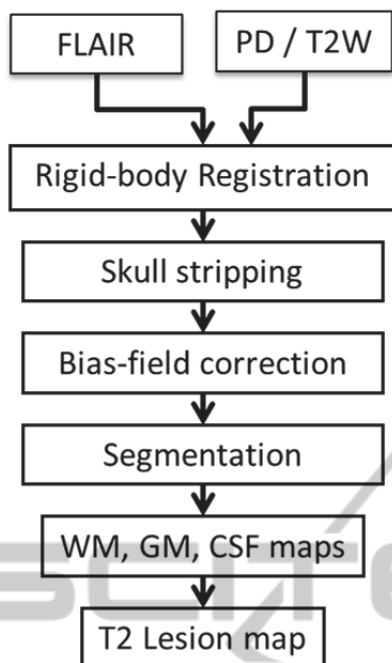


Figure 2: Image analysis pipeline.

removed using an automated procedure that utilizes the fat-saturated T2W images (Datta and Narayana, 2011). Third, the PD, T2W, and FLAIR images were corrected for field nonuniformity using the N4 method (Tustison et al., 2010). Finally, segmentation was performed to classify brain tissue into WM, GM, CSF, and WM lesions using a combination of parametric and nonparametric methods as detailed in (Sajja et al., 2006) and (Datta et al., 2006).

Execution times of the various post-processing and analysis modules and total processing times were recorded for each of the six MS cases studied. Note that the segmentation accuracy was not compromised, and the results obtained from the online pipeline are identical to what would result from off-line processing.

3 RESULTS

Fig. 3 shows one representative dataset at various stages in the analysis pipeline. The corresponding tissue classification is shown in Fig. 4, including WM lesion segmentation. Table 1 reports the processing times used by each of the registration, skull stripping, nonuniformity correction, and segmentation modules, as well as the total processing time. On average, the total processing time is 123 sec. All the six dataset were processed in

under 156 sec, making the results available in almost real-time for the care giver.

4 DISCUSSION

The proposed online image analysis system allows fast computation of quantitative information which was traditionally possible only by performing off-line processing. MS lesions and brain tissues were classified and imported back on the scanner in about two minutes after the acquisition of the data. Importantly, this is achieved without interrupting the scanner workflow with the aid of a dedicated workstation that was seamlessly integrated into the scanner's software.

Having the analysis results immediately after the scan is a valuable contribution to the imaging practice in MS. In addition to quick inspection of the quantitative results and the ability to evaluate data quality while the patient is still in the scanner, the operator can decide on the best flow of the study for each individual case based on the results of

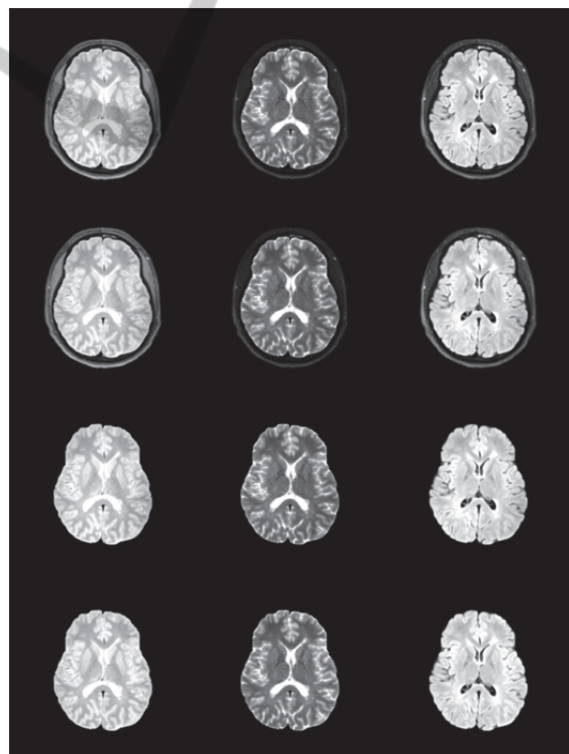


Figure 3: An axial slice from a representative dataset showing the PD (left column), T2W (middle), and FLAIR (right) at different stages of the processing pipeline before (top row) and after (second row) co-registration, after brain extraction (third row), and after nonuniformity correction (fourth row).

Table 1: Execution times (mean \pm standard deviation) for different modules in the online image analysis pipeline measured in six datasets.

Processing module	Time (sec)
Registration	43 \pm 9
Brain extraction	3.2 \pm 0.2
Nonuniformity correction	39 \pm 13
Tissue and lesion segmentation	38 \pm 2
Total time	123 \pm 18

quantitative analysis. The quantitative results can also help determine the optimum parameters for subsequent scans. The proposed online analysis can be applied for online longitudinal evaluation to detect changes in MS lesion activity relative to a previous scan using subtraction MRI, which has shown a potential to predict the course of the disease (Liguori et al., 2011).

Although the 2-min processing time is considerably short compared to the acquisition time of the same data (\sim 8 min), shorter processing times are still desirable, especially when the protocol requires the segmentation results before executing the next imaging sequence. Parallel processing using graphical processing units (GPU) is becoming increasingly popular for medical image analysis (Pratx and Xing, 2011), and will be adopted in future work for further speedup.

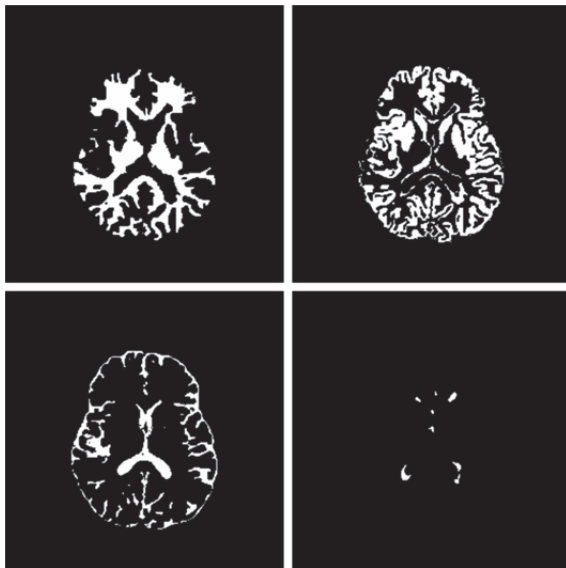


Figure 4: Segmentation results showing masks of white matter (top left), grey matter (top right), CSF (bottom left), and WM lesions (bottom right) corresponding to the slice shown in Fig. 3.

5 CONCLUSIONS

We have developed and implemented an online system for MRI image analysis and demonstrated its application for brain tissue classification and WM lesion segmentation in MS patients. The online image analysis pipeline was integrated into a clinical MRI system that allowed a seamless workflow wherein the results of quantitative analysis were easily incorporated into the patient database and the scanner's user interface. We expect the proposed framework to have an impact on patient management, bringing what has been largely an isolated research activity to be part of the general imaging practice.

ACKNOWLEDGMENTS

The authors thank Vipulkumar Patel for assistance in acquiring the MRI data. This work was supported by NIH/NINDS grant R01 NS078244.

REFERENCES

- Caramanos, Z., Francis, S. J., Narayanan, S., Lapierre, Y. and Arnold, D. L. (2012) 'Large, nonplateauing relationship between clinical disability and cerebral white matter lesion load in patients with multiple sclerosis', *Archives of neurology*, vol. 69, no. 1, p. 89.
- Collignon, A., Maes, F., Delaere, D., Vandermeulen, D., Suetens, P. and Marchal, G. (1995) 'Automated multi-modality image registration based on information theory', *Information processing in medical imaging*, 263-274.
- Datta, S. and Narayana, P. A. (2011) 'Automated brain extraction from T2-weighted magnetic resonance images', *Journal of Magnetic Resonance Imaging*, vol. 33, no. 4, pp. 822-829.
- Datta, S. and Narayana, P.A. (2013) 'A comprehensive approach to the segmentation of multichannel three-dimensional MR brain images in multiple sclerosis', *NeuroImage: Clinical*, vol. 2, pp. 184-196.
- Datta, S., Sajja, B. R., He, R., Wolinsky, J. S., Gupta, R. K. and Narayana, P.A. (2006) 'Segmentation and quantification of black holes in multiple sclerosis', *Neuroimage*, vol. 29, no. 2, p. 467.
- Fisniku, L., Brex, P., Altmann, D., Miszkil, K., Benton, C., Lanyon, R., Thompson, A. and Miller, D. (2008) 'Disability and T2 MRI lesions: a 20-year follow-up of patients with relapse onset of multiple sclerosis', *Brain*, vol. 131, no. 3, pp. 808-817.
- Karimaghloo, Z., Shah, M., Francis, S. J., Arnold, D. L., Collins, D. and Arbel, T. (2012) 'Automatic detection of Gadolinium-enhancing multiple sclerosis lesions in

- brain MRI using conditional random fields', *Medical Imaging, IEEE Transactions on*, vol. 31, no. 6, pp. 1181-1194.
- Kobelt, G., Berg, J., Atherly, D. and Hadjimichael, O. (2006) 'Costs and quality of life in multiple sclerosis A cross-sectional study in the United States', *Neurology*, vol. 66, no. 11, pp. 1696-1702.
- Liguori, M., Meier, D. S., Hildenbrand, P., Healy, B. C., Chitnis, T., Baruch, N.F., Khoury, S.J., Weiner, H.L., Bakshi, R., Barkhof, F. and others (2011) 'One year activity and progression in multiple sclerosis', *Journal of Neurology, Neurosurgery & Psychiatry*, vol. 82, no. 10, pp. 1125-1131.
- Milo, R. and Kahana, E. (2010) 'Multiple sclerosis: geoepidemiology, genetics and the environment', *Autoimmunity reviews*, vol. 9, no. 5, pp. A387--A394.
- Popescu, V., Agosta, F., Hulst, H. E., Sluimer, I.C., Knol, D.L., Sormani, M. P., Enzinger, C., Ropele, S., Alonso, J., Sastre-Garriga, J. and others (2013) 'Brain atrophy and lesion load predict long term disability in multiple sclerosis', *Journal of Neurology, Neurosurgery, and Psychiatry*.
- Pratx, G. and Xing, L. (2011) 'GPU computing in medical physics: A review', *Medical Physics*, vol. 38, p. 2685.
- Sahraian, M. A. and Eshaghi, A. (2010) 'Role of MRI in diagnosis and treatment of multiple sclerosis', *Clinical neurology and neurosurgery*, vol. 112, no. 7, pp. 609-615.
- Sajja, B. R., Datta, S., He, R., Mehta, M., Gupta, R. K. and Wolinsky, J. S. (2006) 'Unified approach for multiple sclerosis lesion segmentation on brain MRI', *Annals of biomedical engineering*, vol. 34, no. 1, pp. 142-151.
- Sweeney, E. M., Shinohara, R. T., Shiee, N., Mateen, F. J., Chudgar, A. A., Cuzzocreo, J. L., Calabresi, P. A., Pham, D. L., Reich, D. S. and Crainiceanu, C. M. (2013) 'OASIS is Automated Statistical Inference for Segmentation, with applications to multiple sclerosis lesion segmentation in MRI', *NeuroImage: Clinical*.
- Tustison, N. J., Avants, B. B., Cook, P. A., Zheng, Y., Egan, A., Yushkevich, P.A. and Gee, J.C. (2010) 'N4ITK: improved N3 bias correction', *Medical Imaging, IEEE Transactions on*, vol. 29, no. 6, pp. 1310-1320.

PRESS
 TECHNOLOGY PUBLICATIONS